Two-Dimensional Superfluid Flows in Inhomogeneous Bose-Einstein Condensates

Zhenya Yan[1],* V. V. Konotop[2], A. V. Yulin[2], and W. M. Liu[3]
[1]*Key Laboratory of Mathematics Mechanization, Institute of Systems Science, AMSS, Chinese Academy of Sciences, Beijing 100190, China*
[2]*Centro de Física Teórica e Computacional and Departamento de Física, Faculdade de Ciências, Universidade de Lisboa, Avenida Professor Gama Pinto 2, Lisboa 1649-003, Portugal*
[3]*Beijing National Laboratory for Condensed Matter Physics, Institute of Physics, Chinese Academy of Sciences, Beijing 100190, China*

We report a novel algorithm of constructing linear and nonlinear potentials in the two-dimensional Gross-Pitaevskii equation subject to given boundary conditions, which allow for exact analytic solutions. The obtained solutions represent superfluid flows in inhomogeneous Bose-Einstein condensates. The method is based on the combination of the similarity reduction of the two-dimensional Gross-Pitaevskii equation to the one-dimensional nonlinear Schrödinger equation, the latter allowing for exact solutions, with the conformal mapping of the given domain, where the flow is considered, to a half-space. The stability of the obtained flows is addressed. A number of stable and physically relevant examples are described.

PACS numbers: 05.45.Yv, 03.75.Lm, 42.65.Tg

I. INTRODUCTION

Nowadays one observes rapidly increasing interest in studying nonlinear Schrödinger (NLS) equations with inhomogeneous coefficients and, in particular, in obtaining their exact analytical solutions for the physically relevant statements. Starting with the first results on integrable inhomogeneous models [1], this activity received further development due to its relevance in nonlinear optics [2] and in the mean-field theory of Bose-Einstein condensates (BECs) [3, 4]. A possibility of constructing exact solutions was also reported for NLS equations with inhomogeneous complex-valued coefficients [5]. However, there are two main limitations of the presently available results. First, most of them were obtained for one-dimensional or quasi-one-dimensional statements and only a few results on multidimensional problems were reported, so far [4, 6]. Second, the most of the models allowing for construction of exact solutions were posed in the infinite domains. The first suggestion of an algorithm for constructing exact solutions of the one-dimensional (1D) NLS equation on a half-line, modeling a BEC interacting with a rigid surface, was recently reported in [7].

Here we show that the requirements of one-dimensionality and unboundness of the domain can be removed and exact analytical solutions can be obtained for models defined on bounded 2D domains and described by the NLS equation with inhomogeneous linear, $V_{\rm ext}(\mathbf{r})$, and nonlinear, $g(\mathbf{r})$, potentials (the both being real-valued functions of the spatial coordinates). Moreover, some of the reported solutions are found to be stable, and thus having particular physical relevance.

The paper is organized as follows. In Sec. II, we present the 2D physical model and give the conformal mapping to reduce the 2D physical model subject to given boundary conditions to nonlinear ordinary differential equation solved. In Sec. III, we concentrate on the two simplest representative examples to illustrate our novel method. Sec. IV is devoted to the numerical simulations for the solutions obtained in the domain D_2. In Sec. V, we study the generalization of the conformal mapping and present exact solutions of the 2D physical model. Finally, the outcomes are summarized in the Conclusion.

II. THE PHYSICAL MODEL AND CONFORMAL MAPPING

To be specific, we deal with the 2D nonlinear physical model

$$i\partial_t\Psi(\mathbf{r},t)=\left[-\frac{1}{2}\nabla^2+V_{\rm ext}(\mathbf{r})+g(\mathbf{r})|\Psi(\mathbf{r},t)|^2\right]\Psi(\mathbf{r},t), \quad (1)$$

where $\mathbf{r}\equiv(x,y)\in D\subset\mathbb{R}^2$, D is an open domain, and $\nabla\equiv(\partial_x,\partial_y)$. We are particularly interested in applications of our results to BEC flows, where $\Psi(\mathbf{r},t)$ is the macroscopic wavefunction and model (1) is also termed, the Gross-Pitaevskii (GP) equation [8]. We explore the flexibility of potentials in the BEC applications, i.e., possibility of manipulating them by external electric and/or magnetic fields for the sake of creation of desirable spatial configurations for the linear potential and for the scattering length of the two-body interactions (the latter performed through the Feshbach resonance technique [9]). We also notice that the model (1) has also direct relevance to the mean-field theory of exciton-polariton condensates [10]. There on the one hand, the 2D statement, i.e. the statement considered in this paper, is the most typical one. On the other hand applying the external pump from the free edges of a specimen one can create

* zyyan_math@yahoo.com

different kinds of nonzero conditions (nonzero currents, as required bellow in the present paper).

We concentrate on a BEC in a domain D bounded by impenetrable walls. Respectively Eq. (1) will be supplied by the zero conditions given at the boundary of the domain D, which we denote as ∂D, i.e., we impose $\Psi(\mathbf{r}) = 0$ for all $\mathbf{r} \in \partial D$.

Our goal is to find an algorithm allowing for systematic constructions of the linear, $V_{\rm ext}(\mathbf{r})$, and nonlinear, $g(\mathbf{r})$, potentials, for which the formulated Dirichlet problem allows for exact analytical solutions. To this aim we assume that there exists a complex analytic function

$$\zeta(\mathbf{r}) \equiv \eta(\mathbf{r}) + i\varphi(\mathbf{r}) = f(z) \tag{2}$$

of the complex variable $z = x+iy \in \mathbb{C}$, which provides the conformal mapping of the contour ∂D to the imaginary axis of $\zeta(\mathbf{r})$, i.e., to $\eta(\mathbf{r}) = 0$, such that the domain D is mapped into the right half-plane in terms of the new variables (η, φ): $\eta(\mathbf{r}) > 0$. Due to analyticity of the mapping $\zeta(\mathbf{r})$ the Cauchy-Riemann equations on the pair of real-valued functions $\eta(\mathbf{r})$ and $\varphi(\mathbf{r})$ hold:

$$\partial_x \eta(\mathbf{r}) = \partial_y \varphi(\mathbf{r}), \quad \partial_y \eta(\mathbf{r}) = -\partial_x \varphi(\mathbf{r}). \tag{3}$$

Respectively, the following constraints

$$\nabla^2 \eta(\mathbf{r}) = 0, \quad \nabla^2 \varphi(\mathbf{r}) = 0, \quad \nabla\eta(\mathbf{r})\cdot\nabla\varphi(\mathbf{r}) = 0 \tag{4}$$

are verified, as well. In other words, $\eta(\mathbf{r})$ and $\varphi(\mathbf{r})$ are both 2D harmonic functions with orthogonal gradients. Moreover, on the basis of the Cauchy-Riemann equations we find the relation $|\nabla\eta(\mathbf{r})|^2 \equiv |\nabla\varphi(\mathbf{r})|^2$.

We restrict the consideration to the linear and nonlinear potentials which can be represented in terms of $\eta(\mathbf{r})$ as follows

$$V_{\rm ext}(\mathbf{r}) \equiv -\frac{\varepsilon}{2}\,|\nabla\eta(\mathbf{r})|^2, \quad g(\mathbf{r}) \equiv \frac{\mathcal{G}}{2}\,|\nabla\eta(\mathbf{r})|^2 \tag{5}$$

where ε and $\mathcal{G}$ are real parameters. Without loss of generality, we choose $\mathcal{G} = \pm 1$. The parameter ε determines the proportionality coefficient between the potentials: $V_{\rm ext}(\mathbf{r})/g(\mathbf{r}) = -\varepsilon/\mathcal{G}$. Then the change of the dependent variables $\Psi(\mathbf{r}, t) \to \psi(\eta, \varphi, t)$, allows one to reduce Eq. (1) to the 2D form

$$i\partial_t \psi = \varrho(\eta, \varphi)\left(-\partial_\eta^2 - \partial_\varphi^2 - \varepsilon + \mathcal{G}|\psi|^2\right)\psi. \tag{6}$$

Here $\varrho(\eta, \varphi)$ is the positive definite function, defined as $\varrho(\eta, \varphi) = |\nabla\eta|^2/2 \equiv |\nabla\varphi|^2/2$, where the gradients must be expressed in terms of η and φ (see the examples below). The obtained equation (6) is considered for $\eta > 0$ and has to be supplied with the zero boundary condition $\psi(\eta = 0, \varphi, t) = 0$.

First, we concentrate on time-independent solutions of Eq. (1): $\Psi(\mathbf{r}, t) \equiv \psi(\eta, \varphi)$, where $\psi(\eta, \varphi)$ solves the 2D stationary GP equation with constant coefficients $\varepsilon\psi = -(\partial_\eta^2 + \partial_\varphi^2)\psi + \mathcal{G}|\psi|^2\psi$. Particular solutions of this equation can be represented as

$$\psi(\eta, \varphi) = e^{i\nu\varphi}\phi(\eta), \tag{7}$$

where ν is a constant and the real-valued function $\phi(\eta)$ solves the problem

$$\mathcal{E}\phi(\eta) = -\partial_\eta^2\phi(\eta) + \mathcal{G}|\phi(\eta)|^2\phi(\eta), \quad \phi(0) = 0, \tag{8}$$

with $\mathcal{E} = \varepsilon - \nu^2$ and $\eta > 0$.

Turning to the physical meaning of the obtained solutions, we observe that it follows from the ansatz, $\psi(\eta, \varphi) = e^{i\nu\varphi}\phi(\eta)$, that $\nabla\varphi(\mathbf{r})$ can be identified as the superfluid velocity. Hence, the introduced analytic function $f(z)$ is nothing but the complex potential of the respective two-dimensional flow. As it is well known [12] such a potential defines the current, J_C of the fluid through a given contour $C \subset D$, as well as the circulation Γ_C along C:

$$\int_C f'(z)dz = \Gamma_C + iJ_C \tag{9}$$

(the prime stands for the derivative with respect to z). Since in our case $f(z)$ is analytic, this integral is zero for any closed contour C bounding a simply connected domain. Thus the described flow has neither sources nor vorticity in D.

We also observe that if the change of variables implies growth of $|\nabla\varphi(\mathbf{r})|$ with $\mathbf{r}$, then the physical meaning might have only solutions with densities decaying at the infinity (thus ensuring decaying currents). Whenever one concerns with finite densities at the infinity, the physically meaningful solutions would correspond to $\nu = 0$. This last constraint is assumed in what follows.

Finally, we notice that if the contour ∂D included in the proposed scheme is closed, this implies that linear and (or) nonlinear potentials are divergent at some point(s) of the boundary. This is clear from the nature of the conformal mapping, since in this case there should be a point of the boundary, which is mapped into the infinity point. In its turn such a point gives an origin to the singularity of the linear and nonlinear potentials. Such cases will be exclude in what follows, although they still may have physical relevance.

III. EXAMPLES OF EXACT SOLUTIONS

While large diversity of the domains can be considered, here we concentrate on the two simplest representative examples for the conformal mapping (2).

A. The quadrant $x > |y|$ with the boundary $x = \pm y$

The first domain considered below, is given by $D_1 = \{x > |y|\}$ (i.e., D_1 is the quadrant of the $(x, y)-$plane) with the boundary $\partial D_1 = \{x = y,\ y > 0\} \cup \{x = -y, y < 0\}$. Respectively, the conformal mapping is chosen as $f(z) = z^2$, and thus $\eta(\mathbf{r}) = x^2 - y^2$ and $\varphi(\mathbf{r}) = 2xy$. The linear and nonlinear potentials are now given by

$$V_{\rm ext}(\mathbf{r}) = -2\varepsilon|\mathbf{r}|^2, \qquad g(\mathbf{r}) = 2\mathcal{G}|\mathbf{r}|^2, \tag{10}$$

i.e., they are the linear expulsive parabolic potential and the parabolic nonlinearity. Now $\varrho(\eta,\varphi) = 2\sqrt{\eta^2+\varphi^2}$.

B. The strip $0 < y < \pi$ with the boundary $y = 0, \pi$

Another domain explored below is a strip $D_2 = \{x \in \mathbb{R},\, 0 < y < \pi\}$ with the boundary $\partial D_2 = \{x \in \mathbb{R},\, y = 0\} \cup \{x \in \mathbb{R},\, y = \pi\}$. Now the function performing conformal mapping to the upper half-plane is $f(z) = e^z$ and the new variables are determined as $\eta(\mathbf{r}) = e^x \sin y$ and $\varphi(\mathbf{r}) = e^x \cos y$. The linear and nonlinear potentials allowing for the exact solutions are now given by

$$V_{\rm ext}(\mathbf{r}) = -2\varepsilon e^{2x}, \qquad g(\mathbf{r}) = 2\mathcal{G}e^{2x}, \tag{11}$$

and $\varrho(\eta,\varphi) = \frac{1}{2}\left(\eta^2+\varphi^2\right)$.

C. Exact solutions

Turning to the exact solutions, below we consider only the case of repulsive interactions $\mathcal{G} = 1$, as the most natural candidate to produce stable stationary flows. As the two simplest solutions of Eq. (1) (see e.g., Refs. [6, 11]) we study, the "dark soliton" shape

$$\Psi_{ds}(\mathbf{r}) = \psi_{ds}(\eta,\varphi) = \sqrt{\mathcal{E}}\tanh\left(\sqrt{\frac{\mathcal{E}}{2}}\,\eta(\mathbf{r})\right) e^{i\nu\varphi(\mathbf{r})} \tag{12}$$

and the nonlinear periodic modulation

$$\Psi_{sn}(\mathbf{r}) = \psi_{sn}(\eta,\varphi) = \frac{k\sqrt{2\mathcal{E}}}{\sqrt{1+k^2}}\,\mathrm{sn}\left(\frac{\sqrt{\mathcal{E}}\,\eta(\mathbf{r})}{\sqrt{1+k^2}}, k\right) e^{i\nu\varphi(\mathbf{r})} \tag{13}$$

with $\mathcal{E} = \varepsilon - \nu^2 > 0$ and $k \in (0,\,1]$ being the modulus of the Jacobi elliptic sn–function [notice that $\psi_{ds}(0,\varphi) = \psi_{sn}(0,\varphi) = 0$, in conformity with the imposed boundary conditions]. These exact solutions given by Eqs. (12) and (13) and the corresponding velocity fields in the domains D_1 and D_2 are illustrated in Fig. 1.

The obtained exact solutions, however leave several open questions related to their practical feasibility. First, the stability of the flows was not investigated, so far. Second, in all considered cases infinitely growing potentials were used, while any cut-off (which exists in the real world) may strongly perturb, and even destroy the solutions. To address these issues we now turn to direct numerical simulations.

In the case at hand the potentials $V_{\rm ext}(\mathbf{r})$ and $g(\mathbf{r})$ grow with x, while the density goes asymptotically to (or is bounded by) a certain constant level. Bearing this in mind we construct a physical system with bounded potential in the following way. For $x < 0$ we consider shifted linear and nonlinear potentials $V_{\rm ext}(\mathbf{r}-\mathbf{r}_0)$ and $g(\mathbf{r}-\mathbf{r}_0)$, where $\mathbf{r}_0 = (x_0, 0)$ with x_0 being a constant shift vector, while $V_{\rm ext}(\mathbf{r})$ and $g(\mathbf{r})$ are given by the analytical formulas (5). To define the physical potentials at $x > 0$ we mirror them at $x = 0$, thus obtaining $V_{\rm ext}(-\mathbf{r}+\mathbf{r}_0)$ and $g(-\mathbf{r}+\mathbf{r}_0)$. To confine the condensate along y-coordinate we introduce additional linear tarp potential as follows: $v_{add} = 0$ for $\mathbf{r} \in D$ and $v_{add} = V_0$, where V_0 is large enough, for $\mathbf{r} \notin D$. For more details see the next chapter where we discuss the numerical studies of the problem.

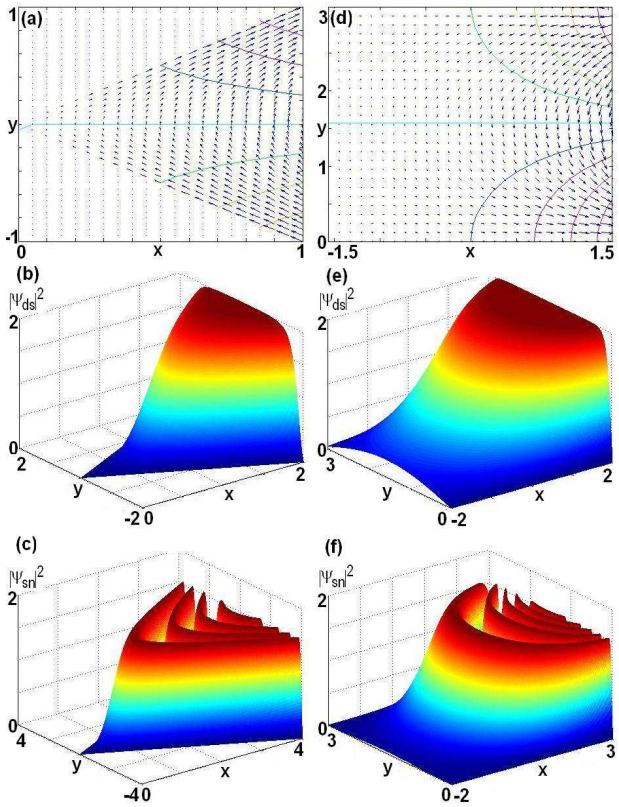

FIG. 1. (color online). The profiles for exact solutions given by Eqs. (12) and (13) and the corresponding velocity fields in the domains D_1 and D_2. Left column: Panels (a), (b), (c) show the velocity field $\nabla\varphi(\mathbf{r}) = (2y, 2x)$, and densities $|\Psi_{ds}(\mathbf{r})|^2$ and $|\Psi_{sn}(\mathbf{r})|^2$ for solutions given by (12) and (13) in the domain D_1. Right column: Panels (d), (e), (f) show the velocity field $\nabla\varphi(\mathbf{r}) = (e^x\cos y, e^x \sin y)$, and densities $|\Psi_{ds}(\mathbf{r})|^2$ and $|\Psi_{sn}(\mathbf{r})|^2$ for solutions given by (12) and (13) in the domain D_2. The parameters are $\varepsilon = 2$, $\nu = 0$, and $k = 0.8$.

IV. DIRECT NUMERICAL SIMULATIONS

Now we can perform direct numerical simulations of Eq. (1) with the additional confining potential v_{add} taking the initial distribution of the field in the form given by the analytical formulas $\psi(\mathbf{r}-\mathbf{r}_0)$ for $x < 0$ and $\psi(\mathbf{r}_0-\mathbf{r})$ for $x > 0$. As it is clear our ansatz does not satisfy Eq. (1) only along the line $x = 0$ and in the areas $y < 0$ and $y > \pi$. Since, however we impose strong confining potential, we expect that the field is very weak outside the stripe $0 < y < \pi$ and our ansatz stays sufficiently close to the real stationary solution of Eq. (1) with the introduced physical potentials. The analytically found

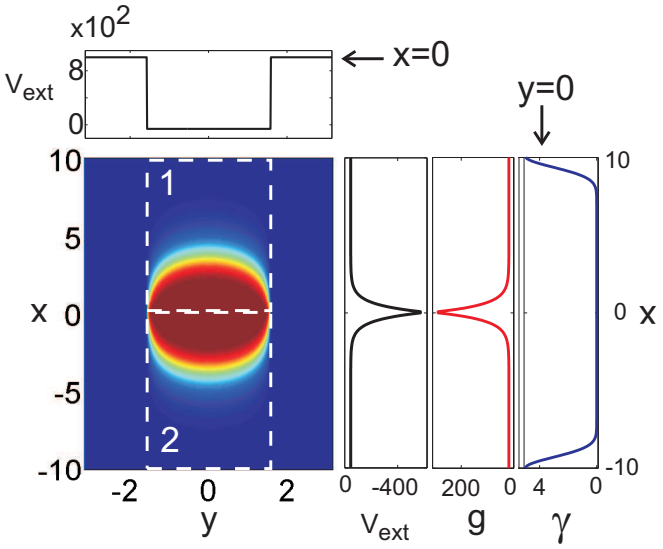

FIG. 2. (color online). The ansatz produced from the solutions the with parameters $\varepsilon = 2$, $\nu = 0$. In the upper part of the figure the distribution of the linear potential along y is shown for $x = 0$. On the right the distributions of the linear and nonlinear potentials are shown alongside with the introduced loss for $y = 0$. In the areas marked by "1" and "2" the anzatz exactly coincides with the analytical solution (neglecting exponentially weak loss).

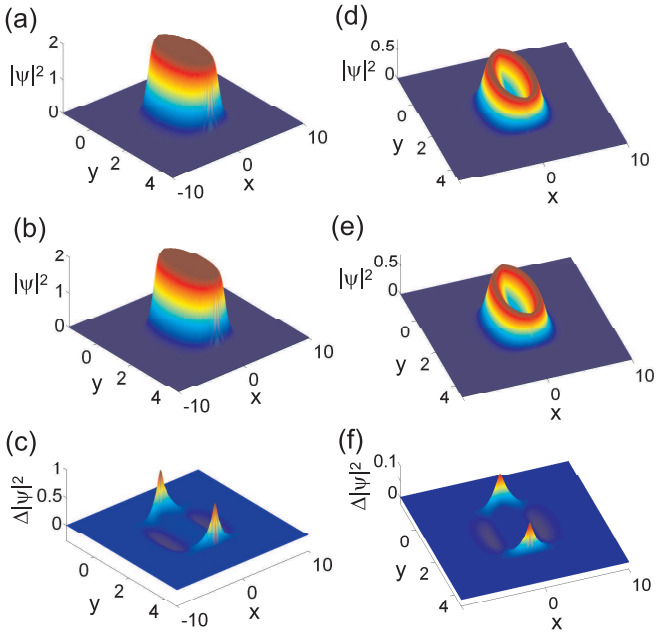

FIG. 3. (color online). Panels (a) and (d) show the initial distribution of the density of the condensates for cases 1 and 2; panels (b) and (e) show the distributions of the condensate densities at $t = 100$; panels (c)and (f) show the differences between the initial density distributions and the density distributions at $t = 100$. The shifts of the initial conditions and the potentials are $x_0 = -2.5$ for (a)-(c) and $x_0 = -2$ for (d)-(f). The solution parameters are $\varepsilon = 2$, $\nu = 0$. The field is kept within the stripe by strong repelling linear potential $v_a = 10^4$ for $y < 0$ and $y > \pi$. The parameters for the linear losses are $\gamma_0 = 5$, $w_0 = 1$, $x_l = 10$.

solution and the corresponding potentials are shown in Fig. 2. Within the areas "1" and "2" the ansatzes used in the numerics as the initial condition coincides with the analytical solutions. However on the boundary between these areas the ansatzes do not satisfy the equation for stationary fields. The ansatz does not satisfy the equation outside the areas either. However the density of the condensate is low outside the areas and so there are some reasons to believe that the ansatz is close to the stationary solution. Let us remind here that in our numerical simulations to keep the condensate localized within the stripe we used strong linear potential, see the distribution of the linear potential along y.

We carried out numerical simulations for the solutions obtained in the domain D_2 and found out that some non-stationary excitations appear but the solution survive and stay rather close to the initial field distribution. To check the stability of the solution for longer time we had to get rid of the propagating excitations. Since we perform numerical simulations in finite windows the only way to eliminate the propagating excitations is to introduce losses in the area where initially the density of the condensate is exponentially weak. To do this we introduce linear losses in the form $\gamma = \gamma_0 \left[\exp(-(x - x_l)^2/w_0^2) + \exp(-(x + x_l)^2)/w_0^2\right]$. Then the losses are negligible in the area where our analytical solution is big and so the solution is practically unaffected by the artificial losses used in the numerics. In the same time all the perturbations propagating away are quickly absorbed. In this case the excitations disappear very quickly and one can see in Fig. 3 that the surviving solution is very close to the initial distribution. As it is expected the stationary solution deviates from the ansatz most strongly around the points $(x = 0,\ y = 0)$ and $(x = 0,\ y = \pi)$.

In the case of attractive interactions (of a negative scattering length) the solution appears to be unstable against collapse.

V. THE GENERALIZED CONFORMAL MAPPING

Next we address possibilities of getting more general types of the potentials, allowing for exact solutions. To this end we introduce the generalized relations [c.f. the Cauchy-Riemann equations (3)]:

$$\rho^2(\hat{\eta})\partial_x\hat{\eta}(\mathbf{r}) = \partial_y\hat{\varphi}(\mathbf{r}),\ \ \rho^2(\hat{\eta})\partial_y\hat{\eta}(\mathbf{r}) = -\partial_x\hat{\varphi}(\mathbf{r}), \quad (14)$$

where $\rho^2(\hat{\eta})$ is a positive-definite function of $\hat{\eta}(\mathbf{r})$ only [as it is clear the arguments presented below can be also applied to the case where $\rho^2(\hat{\varphi})$ is a function of $\hat{\varphi}(\mathbf{r})$ only]. These equations still define transformation to the orthogonal coordinates $(\hat{\eta}, \hat{\varphi})$, however now satisfying the

relations [c.f. Eq. (4)]

$$\nabla\cdot[\rho^2(\hat{\eta})\nabla\hat{\eta}]=0,\ \nabla\cdot[\rho^2(\hat{\eta})\nabla\hat{\varphi}]=0,\ \nabla\hat{\eta}\cdot\nabla\hat{\varphi}=0. \quad (15)$$

Moreover, now we have that $|\nabla\hat{\varphi}(\mathbf{r})|^2 \equiv \rho^4(\hat{\eta})|\nabla\hat{\eta}(\mathbf{r})|^2$. Notice that the generalized case [c.f. Eq. (15)] can be reduced to the case mentioned above [c.f. Eq. (4)] in the special case $\rho^2(\hat{\eta})\equiv 1$.

Next we repeat the steps described above for the conformal mapping, and by the direct algebra show that the generalized ansatz

$$\psi(\hat{\eta},\hat{\varphi})=\rho(\hat{\eta})e^{i\nu\hat{\varphi}(\mathbf{r})}\phi[\hat{\eta}(\mathbf{r})] \quad (16)$$

solves the 2D stationary GP equation (1) provided that $\phi(\mathbf{r})$ satisfy the stationary equation (8) with $\eta(\mathbf{r})$ substituted by $\hat{\eta}(\mathbf{r})$ and the linear and nonlinear potentials are given by

$$\begin{aligned} V_{\rm ext}(\mathbf{r}) &\equiv \frac{\nabla^2\rho}{2\rho}+\frac{\nu^2(1-\rho^4)-\varepsilon}{2}|\nabla\hat{\eta}|^2, \\ g(\mathbf{r}) &\equiv \frac{\mathcal{G}|\nabla\hat{\eta}|^2}{2\rho^2}. \end{aligned} \quad (17)$$

Notice that now the linear and nonlinear potentials are not proportional to each other any more [c.f. Eq. (5)].

To construct a particular example, we choose

$$\hat{\eta}(\mathbf{r})=2\eta(\mathbf{r})+\frac{\eta^2(\mathbf{r})}{2},\ \hat{\varphi}(\mathbf{r})=\varphi(\mathbf{r}),\ \rho(\hat{\eta})=\frac{1}{\sqrt{2+\eta(\mathbf{r})}} \quad (18)$$

with $\eta(\mathbf{r})$ and $\varphi(\mathbf{r})$ solving Eq. (4). One can ensure that this choice also satisfies the conditions (15). Then the simplest solution of Eq. (8) with the repulsive nonlinearity ($\mathcal{G}=1$) is given by we study, the "dark soliton" shape (12) with $\eta(\mathbf{r})$ substituted by $\hat{\eta}(\mathbf{r})$ and valid for the positive chemical potential $\mathcal{E}=\varepsilon-\nu^2>0$.

Then, according to the generalized ansatz with $\hat{\eta}(\mathbf{r})$, $\hat{\varphi}(\mathbf{r})$, and $\rho(\hat{\eta})$ given by Eq. (18), as well as $\eta(\mathbf{r})$ and $\varphi(\mathbf{r})$ defined in the domain D_2, we obtain the "dark soliton"

$$\hat{\psi}_{ds}(\mathbf{r})=\sqrt{\mathcal{E}}\rho(\hat{\eta})\tanh\left(\sqrt{\frac{\mathcal{E}}{2}}\hat{\eta}(\mathbf{r})\right)\exp(i\nu e^x\cos y), \quad (19)$$

with $\eta\equiv\eta(\mathbf{r})=e^x\sin y$, which solves Eq. (1) with the linear and nonlinear potentials given by [c.f. Eq. (17)]

$$\begin{aligned} V_{\rm ext}(\mathbf{r}) &= \frac{e^{2x}}{8(2+\eta)^2}\big\{3-16(4\mathcal{E}+\nu^2)-2\eta\big[\nu^2(3+2\eta) \\ &\quad +2\mathcal{E}(4+\eta)(\eta^2+4\eta+8)\big]\big\}, \\ g(\mathbf{r}) &= \frac{1}{2}e^{2x}(2+\eta)^3. \end{aligned}$$

The presented solutions found in the domain D_2 behave in a way similar to the previous example, see Fig. 3. The numerical simulations prove that the found analytical solutions can indeed be used as good approximation for the stable stationary solutions of Eq. (1) describing systems with physically relevant potentials.

VI. CONCLUSION

To conclude, we have shown that exact analytical solutions can be obtained in a large class of two-dimensional Gross-Pitaevskii equations with inhomogeneous linear and nonlinear potentials, defined on bounded domains. The method of constructing the models is based on the properly defined conformal mapping of the given domain into a complex half-plane. In the context of applications to Bose-Einstein condensates, the obtained solutions having nontrivial phase depending on spatial coordinates can be interpreted as superfluid flows. In the case of negative scattering length (repulsive interactions) the background flows, i.e., ones having no zeros in the open spatial domain, appear to be stable. The obtained results generalize previous studies devoted to construction of the exact solutions, using the self-similar transformation, to the two-dimensional models given on bounded domains. Moreover, the ideas presented in this paper are also able to apply in two-dimensional cubic-quintic models, two-dimensional multi-component models, etc., and to design linear and nonlinear potentials for control of Bose-Einstein condensates and nonlinear optical fibers in limited spatial domains.

ACKNOWLEDGMENTS

Yan was supported by the NSFC under Grant No. 11071242. VVK and AVY were supported by the grant PEst-OE/FIS/UI0618/2011 and by 7th European Community Framework Programme under the grant PIIF-GA-2009-236099 (NOMATOS). Liu was supported by the NKBRSFC under Grant No. 2011CB921502.

[1] H.-H. Chen and C.-S. Liu, Phys. Rev. Lett. **37**, 693 (1976); M. Bruschi, D. Levi, and O. Ragnisco, Il Nuovo Cimento A **53**, 21 (1979); R. Scharf and A. R. Bishop, Phys. Rev. A **43**, 6535 (1991); V. V. Konotop, O. A. Chubykalo, and L. Vázquez, Phys. Rev. E **48**, 563 (1993); L. Gagnon and P. Winternitz, J. Phys. A **26**, 7061 (1993); V. V. Konotop, Theor. Math. Phys. **99**, 687 (1994).

[2] V. N. Serkin, and A. Hasegawa, Phys. Rev. Lett. **85**, 4502 (2000); B. A. Malomed *et al.*, J. Opt. B: Quantum Semiclass. Opt. **7**, R53 (2005); S. A. Ponomarenko and G. P. Agrawal, Phys. Rev. Lett. **97**, 013901 (2006); V. N. Serkin, A. Hasegawa, and T. L. Belyaeva, Phys. Rev.

Lett. **98**, 074102 (2007); Z. Y. Yan, Phys. Lett. A **374**, 672 (2010).
[3] Z. X. Liang, Z. D. Zhang, and W. M. Liu, Phys. Rev. Lett. **94**, 050402 (2005); J. Belmonte-Beitia *et al.,* Phys. Rev. Lett. **98**, 064102 (2007); J. Belmonte-Beitia *et al.,* Phys. Rev. Lett. **100**, 164102 (2008); A. T. Avelar, D. Bazeia, and W. B. Cardoso, Phys. Rev. E **79**, 025602(R) (2009).
[4] V. M. Pérez-García, P. J. Torres, and V. V. Konotop, Physica D **221**, 31 (2006).
[5] F. Kh. Abdullaev *et al.*, Phys. Rev. E **82**, 056606 (2010).
[6] Z. Y. Yan and V. V. Konotop, Phys. Rev. E **80**, 036607 (2009); Z. Y. Yan and C. Hang, Phys. Rev. A **80**, 063626 (2009); S. H. Chen and J. M. Dudley, Phys. Rev. Lett. **102**, 233903 (2009); Z. Y. Yan, V. V. Konotop, and N. Akhmediev, Phys. Rev. E **82**, 036610 (2010); Z. Y. Yan, Phys. Scr. **78**, 035001 (2008); Z. Y. Yan, Phys. Lett. A **374**, 4838 (2010); Z. Y. Yan, K. W. Chow, and B. A. Malomed, Chaos, Solitons & Fractals, **42**, 3013 (2009).
[7] Yu. V. Bludov, Z. Y. Yan, and V. V. Konotop, Phys. Rev. A **81**, 063610 (2010).
[8] F. Dalfovo *et al.*, Rev. Mod. Phys. **71**, 463 (1999).
[9] P. O. Fedichev *et al.*, Phys. Rev. Lett. **77**, 2913 (1996).
[10] A. Amo, D. Sanvitto, F. P. Laussy, D. Ballarini1, E. del Valle, M. D. Martin1, A. Lemaître, J. Bloch, D. N. Krizhanovskii, M. S. Skolnick, C. Tejedor, and L. Viña Nature, **457**, 291 (2009); A. Amo, T. C. H. Liew, C. Adrados, R. Houdré , E. Giacobino, A. V. Kavokin and A. Bramati Nature Photonics, **4**, 361 (2010).
[11] L. D. Faddeev and L. A. Takhtajan, *Hamiltonian Methods in the Theory of Solitons* (Springer-Verlag, Berlin, 1987).
[12] see e.g. A. J. Majda and A. L. Bertozzi, *Vorticity and Incompressible Flow* (Cambridge University Press, 2002).